Zero : Jurnal Sains. Matematika. dan Terapan
E-ISSN : 2580-5754; P-ISSN : 2580-569X
Volume 10 Number 2. 2026
DOI: 10.30829/zero.v10i2.30511
Page: 614-624

Modelling Leptospirosis Transmission with Waning Immunity and Stage-Structured Infection: Local stability and Vaccination Analysis

[1]Dinta Ardelia Wahyudi
Department of Mathematics, Universitas Negeri Surabaya, Surabaya, 60231, Indonesia

[2]Budi Priyo Prawoto
Department of Mathematics, Universitas Negeri Surabaya, Surabaya, 60231, Indonesia

Article Info

Article history:

Accepted: 10 July 2026

Keywords:

Basic reproduction number;
Leptospirosis;
Routh-Hurwitz;
Stage-structured model;
Vaccination.

ABSTRACT

Leptospirosis remains a complex zoonotic threat. This study develops a stage-structured mathematical model of leptospirosis transmission incorporating vaccine-induced immunity and two-stage treatment. The basic reproduction number (R_0), derived via the Next-Generation Matrix method, serves as a threshold where $R_0 < 1$ indicates disease elimination, whereas $R_0 > 1$ indicates persistence, with equilibrium stability analyzed using the Routh-Hurwitz criterion. To evaluate controls, we explicitly contrast two parameter regimes: a disease-free scenario under high interventions and reduced contact rates ($f = 0.80$, $\theta = 0.40$, $\beta_h = 0.10$) resulting in $R_0 = 0.7696$, and an endemic scenario with low interventions and a high contact rate ($f = 0.15$, $\theta = 0.10$, $\beta_h = 0.66$) yielding $R_0 = 6.009$. Vaccination and awareness alone cannot eliminate the disease; reducing human-vector contact rates (β_h) through environmental control is strictly required. Combining 80% vaccination and 40% awareness with these environmental measures reduces transmission potential by 88%, providing quantifiable public health policies.

Corresponding Author:

Budi Priyo Prawoto,
Department of Mathematics,
Universitas Negeri Surabaya
Email: budiprawoto@unesa.ac.id

1. INTRODUCTION

Leptospirosis is a zoonotic infectious disease caused by pathogenic Leptospira bacteria and remains a major public health concern, particularly in tropical and developing regions [1]. The disease is primarily transmitted through contact with water or soil contaminated by the urine of infected animals, predominantly rat vectors, where environmental factors play a crucial role in maintaining disease transmission [2], [3], [4], [5]. Due to its complex transmission pathways involving environmental reservoirs and human-rodent interactions, leptospirosis remains difficult to control using a single intervention strategy.

In Indonesia, leptospirosis remains a major public health burden driven by favorable climate, abundant rodent populations, and frequent flooding. Ministry of Health data show high case fatality rates exceeding 9% annually, with 1,170 cases (106 deaths) in 2020, 734 cases (84 deaths) in 2021, and 1,419 cases (139 deaths) in 2022 [6], [7]. The disease is widely distributed across several provinces, including East Java, Central Java, Yogyakarta, Banten, DKI Jakarta, and East Kalimantan [8]. Recurrent flooding events further escalate outbreak risks by increasing human exposure to water contaminated by infected animal urine [7], [9]. This high mortality and persistent transmission highlight the urgent need for effective, sustainable intervention strategies to mitigate the disease's impact.

Mathematical modeling is widely utilized to analyze the transmission dynamics of infectious diseases, including leptospirosis [1], [10]. To evaluate disease persistence and control, several studies have explicitly incorporated environmental reservoirs to represent the survival of Leptospira in contaminated water or soil [5], [11], [12]. Furthermore, integrating ecological, demographic, and intervention-related factors has been shown to improve a model's capacity to represent transmission dynamics and assess potential control strategies [12], [13], [14]. Although these approaches enhance our epidemiological understanding through diverse biological mechanisms, the optimal model structure remains highly dependent on the specific objectives and underlying assumptions of each study.

While existing models typically isolate control strategies [10], [11], [15] and represent infection as a single stage [16], [17] failing to capture how active early-stage individuals contribute to transmission while hospitalized severe-stage patients do not this study proposes a unified leptospirosis model integrating temporary vaccination, stage-structured human infection, and asymmetric human–rat transmission. Unlike the leptospirosis transmission models proposed by Eguda et al. [1] and Engidaet al. [4], which represent human infection using a single infectious compartment, the present study explicitly distinguishes early- and severe-stage infections. Furthermore, the proposed framework incorporates temporary vaccination with waning immunity into the stage-structured transmission model, providing a unified framework for analyzing vaccination and disease progression. Furthermore, since human leptospirosis vaccination is not routine in Indonesia and remains limited globally by its temporary, serovar-specific protection, the vaccination compartment represents a hypothetical scenario; this allows the study to establish a theoretical framework to evaluate how temporary immunity, if available, would interact with stage-specific progression to influence transmission, rather than reflecting current public health practices.

This study presents a stage-structured leptospirosis model with vector dynamics and temporary vaccine immunity, partitioning humans (susceptible, vaccinated, exposed, two-stage infected, recovered) and vectors (susceptible, infected). We analytically derive the disease-free and endemic equilibria, calculate R_0, and prove their local stability. Numerical simulations illustrate qualitative dynamics under various intervention regimes, offering theoretical insights into combining temporary immunization and stage-specific treatments for integrated disease control.

2. RESEARCH METHOD

2.1 Model Structure

The leptospirosis framework models the dynamical interactions between human hosts (N_h) and rat vectors (N_v). Rather than utilizing an explicit compartment, the environmental reservoir is implicitly incorporated into the transmission coefficients (β_h and β_v), which directly account for the long-term persistence and survival of Leptospira in soil and water. The human population is divided into six compartments: vaccinated (V_h), susceptible (S_h), exposed (E_h), first-stage infected (I_1), second-stage infected with severe clinical symptoms (I_2), and recovered (R_h), such that $N_h(t) = V_h(t) + S_h(t) + E_h(t) + I_1(t) + I_2(t) + R_h(t)$. Meanwhile the rat vector population consists of susceptible (S_v) and infected (I_v) compartments, with total population $N_v(t) = S_v(t) + I_v(t)$.

Based on [1], [10], [18] the model assumes constant natural recruitment for both populations, with a proportion of human newborns vaccinated immediately. This vaccine-induced immunity is temporary, eventually returning individuals to the susceptible class. Host-vector transmission is indirect, asymmetric, and implicitly environmental: humans acquire infection from contaminated water or soil (mitigated by public awareness), while susceptible rats are infected solely by pathogens shed by early-stage infected humans (I_1). Sequentially, exposed humans progress through the exposed (E_h), first-stage (I_1), and second-stage (I_2) compartments. Only I_1 individuals contribute to environmental contamination; hospitalized or isolated I_2 patients have a negligible transmission impact [19], [20]. Early-stage individuals (I_1)either recover or progress to the severe stage (I_2). Natural mortality applies to all compartments, whereas disease-induced mortality is restricted to infected humans and rats. Lastly, recovered humans eventually lose natural immunity, while infected rats remain infectious until death, as illustrated in Figure 1.

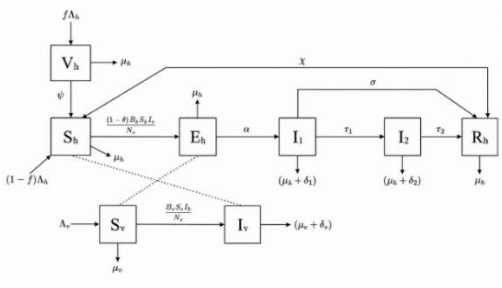

Figure 1. Compartmental Diagram of Model.

2.2 Differential Equation System

Based on the compartment structure and the biological assumptions, leptospirosis transmission dynamics are formulated by the following system of differential equations:

$$\frac{dV_h}{dt} = f\Lambda_h - (\psi + \mu_h)V_h \quad (1)$$

$$\frac{dS_h}{dt} = (1-f)\Lambda_h + \psi V_h + \chi R_h - \mu_h S_h - \frac{(1-\theta)\beta_h S_h I_v}{N_v} \quad (2)$$

$$\frac{dE_h}{dt} = \frac{(1-\theta)\beta_h S_h I_v}{N_v} - (\mu_h + \alpha)E_h \quad (3)$$

$$\frac{dI_1}{dt} = \alpha E_h - (\mu_h + \delta_1 + \tau_1 + \sigma)I_1 \quad (4)$$

$$\frac{dI_2}{dt} = \sigma I_1 - (\mu_h + \delta_2 + \tau_2)I_2 \quad (5)$$

$$\frac{dR_h}{dt} = \tau I_1 + \tau I_2 - (\chi + \mu_h)R_h \quad (6)$$

$$\frac{dS_V}{dt} = \Lambda_v - \mu_v S_v - \frac{\beta_v S_v I_1}{N_h} \quad (7)$$

$$\frac{dI_V}{dt} = \frac{\beta_v S_v I_1}{N_h} - (\mu_v + \delta_v)I_v \quad (8)$$

All model parameters are assumed to be non-negative, with their detailed descriptions summarized in Table 1.

Table 1. Parameter Description

Parameter	Description
Λ_h	Birth or recruitment rate of human
μ_h	Natural death rate of all human subclasses
ψ	Waning rate of temporary immunity of the vaccinated human
f	Proportion of vaccinated against leptospirosis disease
β_h	Effective contact rate for leptospirosis from vector to human
β_v	Effective contact rate for leptospirosis from human to vector
α	Progression rate of carrier human into infective subclass
σ	Rate of disease progression
τ_1	Recovery rate of human with first stage leptospirosis
τ_2	Recovery rate of human with second stage leptospirosis
δ_1	First-stage disease-induced mortality rate
δ_2	Second-stage disease-induced mortality rate
δ_v	Death rate of vector due to leptospirosis disease
χ	Waning rate of natural immunity
θ	Compliance rate to public awareness campaign
Λ_v	Birth or recruitment rate of vector
μ_v	Natural death rate of the vector

2.3 Equilibrium Point

The long-term dynamics of the proposed leptospirosis model are governed by its equilibrium points [4], [21], [22]. The disease-free equilibrium (DFE), representing complete infection eradication obtained by setting all infected compartments to zero, and the endemic equilibrium (EE), indicating permanent disease persistence evaluated under steady-state propagation.

2.4 Basic Reproduction (R_0)

The basic reproduction number (R_0) measures the average secondary infections caused by a single infected individual in a fully susceptible population [23], [24]. In this study, the explicit formula for R_0 is analytically derived from the DFE using the next-generation matrix method [8]. This threshold dictates that the disease dies out asymptotically if $R_0 < 1$, but has the potential to become endemic if $R_0 > 1$ [25].

2.5 Sensitivity Analysis of R_0

To evaluate how individual parameters drive or mitigate the outbreak, a local sensitivity analysis is performed on the basic reproduction number (R_0). Using the normalized forward sensitivity index (elasticity index), the relative change in R_0 with respect to a parameter p is formulated as:

$$\Upsilon_p^{R_0} = \frac{\partial R_0}{\partial p} \times \frac{p}{R_0}$$

This formulation analytically determines the influence of all R_0 parameters prior to numerical evaluation.

2.6 Linearization & Stability Analysis

To evaluate local asymptotic stability, the non-linear system (1)–(8) is linearized using the Jacobian matrix $J(X)$ [26]. System stability is determined by the signs of the eigenvalues from the characteristic equation $|J(X) - \lambda I| = 0$. Since the two-stage infection structure (I_1 and I_2) yields a higher-order characteristic polynomial, deriving explicit analytical eigenvalues is highly complex. To circumvent this, the Routh-Hurwitz criterion is applied to verify that all roots possess strictly negative real parts without requiring explicit calculations [27].

2.7 Numerical Simulation

Numerical simulations are performed in MATLAB using the fourth-order Runge-Kutta method to solve the differential system (1)–(8), validating the analytical stability results and visualizing trajectory dynamics [28]. By utilizing literature-sourced parameter values, these computational experiments evaluate two primary epidemiological scenarios ($R_0 < 1$ and $R_0 > 1$). Ultimately, the simulations illustrate the dynamic impact of public health interventions, focusing specifically on human vaccination efficiency and severe-case isolation.

3. RESULT AND ANALYSIS

3.1 Equilibrium Point

The equilibrium points of the proposed leptospirosis transmission model are determined by setting all first order differential equations to zero:

$$\frac{dV_h}{dt} = \frac{dS_h}{dt} = \frac{dE_h}{dt} = \frac{dI_1}{dt} = \frac{dI_2}{dt} = \frac{dR_h}{dt} = \frac{dS_V}{dt} = \frac{dI_V}{dt} = 0$$

These steady states dictate whether the disease will ultimately disappear or permanently persist within the population [10]. By setting all infected compartments to zero ($E_h = I_1 = I_2 = R_h = I_v = 0$), the disease-free equilibrium (DFE) is obtained as:

$$E^0 = \left(\frac{f\Lambda_h}{(\psi + \mu_h)}, \frac{\Lambda_h(\psi + \mu_h - f\mu_h)}{\mu_h(\psi + \mu_h)}, 0,0,0,0, \frac{\Lambda_v}{\mu_v}, 0\right)$$

Given that the vaccination fraction satisfies $0 \leq f \leq 0$, the term $\psi + \mu_h(1-f)$ is strictly positive. This condition guarantees $S_h^0 > 0$ across all biological parameter values, ensuring the DFE remains biologically meaningful and represents a complete interruption of the transmission chain [13].

Furthermore, if the disease persists in the population, the endemic equilibrium point is obtained and denoted by $E^* = (V_h{}^*, S_h{}^*, E_h{}^*, I_1{}^*{}_1, I_2{}^*, R_h{}^*, S_v{}^*, I_v{}^*)$ where :

$$\mathrm{V_h^*} = \frac{f\Lambda_h}{(\psi+\mu_h)};\ S_h{}^* = \frac{(\mu_h+\alpha)(\mu_h+\delta_1+\tau_1+\sigma)\left[\frac{\Lambda_h(\mu_v+\delta_v)}{\mu_h}+\left(\beta_v-\frac{\mu_v+\delta_v}{\mu_h}\left(\delta_1+\frac{\sigma\delta_2}{\mu_h+\delta_2+\tau_2}\right)\right)I_1^*\right]}{\alpha(1-\theta)\beta_h\beta_v};\ E_h^* = \frac{(\mu_h+\delta_1+\tau_1+\sigma)}{\alpha}I_1^*;$$

$$I_1^* = \frac{\left[\frac{(\mu_h+\alpha)(\mu_h+\delta_1+\tau_1+\sigma)}{\alpha}\right](\mu_h+\delta_v)\left(\frac{\Lambda_h}{\mu_h}\right)-\left[\frac{\Lambda_h(\psi+\mu_h-f\mu_h)}{\mu_h(\psi+\mu_h)}\right](1-\theta)\beta_h\beta_v}{\left[\left(\frac{\chi\tau(\mu_h+\delta_2+\tau_1+\sigma)}{(\chi+\mu_h)(\mu_h+\delta_2+\tau_2)}-\frac{(\mu_h+\alpha)(\mu_h+\delta_1+\tau_1+\sigma)}{\alpha}\right)\frac{(1-\theta)\beta_h}{\mu_h}-\frac{(\mu_h+\alpha)(\mu_h+\delta_1+\tau_1+\sigma)}{\alpha}\right]\beta_v+\frac{(\mu_h+\alpha)(\mu_h+\delta_1+\tau_1+\sigma)(\mu_v+\delta_v)}{\alpha\mu_h}\left[\delta_1+\frac{\sigma\delta_2}{\mu_h+\delta_2+\tau_2}\right]};$$

$$I_2^* = \frac{\sigma I_1^*}{\mu_h+\delta_2+\tau_2};\ R_h^* = \frac{\tau}{\chi+\mu_h}\left(1+\frac{\sigma}{\mu_h+\delta_2+\tau_2}\right)I_1^*;\ S_v^* = \frac{\Lambda_v\left[\left(\frac{\Lambda_h}{\mu_h}-\frac{1}{\mu_h}\left(\delta_1+\frac{\sigma\delta_2}{\mu_h+\delta_2+\tau_2}\right)I_1^*\right)\right]}{\mu_v\left[\mu_h\left(\frac{\Lambda_h}{\mu_h}-\frac{1}{\mu_h}\left(\delta_1+\frac{\sigma\delta_2}{\mu_h+\delta_2+\tau_2}\right)I_1^*\right)+\beta_v I_1^*\right]};$$

$$I_v^* = \frac{\beta_v \Lambda_v I_1^*}{(\mu_v + \delta_v)\left[\mu_v\left(\frac{\Lambda_h}{\mu_h} - \frac{1}{\mu_h}\left(\delta_1 + \frac{\sigma\delta_2}{\mu_h + \delta_2 + \tau_2}\right)I_1^*\right) + \beta_v I_1^*\right]}$$

If the infection persists, the endemic equilibrium (E^*) is obtained, signifying permanent disease persistence driven by continuous host-vector interactions [3], [29]. The mathematical validity of the coordinate components for E^* is verified via direct substitution into the state equations (1)-(8) under steady-state conditions. Crucially, only first-stage infected individuals (I_1) contribute to vector transmission, as severe second stage individuals (I_2) are assumed to be isolated or hospitalized, preventing further vector contact [16]. The local asymptotic stability of these steady states is evaluated using the Jacobian matrix and the Routh–Hurwitz criterion, establishing that the DFE stable if $R_0 < 1$, while E^* exists and stabilizes when $R_0 > 1$ [15], both of which are subsequently validated via numerical simulations.

3.2 Local Stability of Disease-Free & Endemic Equilibria

The disease-free equilibrium (E^0) is locally asymptotically stable if all eigenvalues of its corresponding Jacobian matrix possess strictly negative real parts. Biologically, this stability ensures the system suppresses minor epidemiological perturbations, allowing the population to return to a completely healthy state. These eigenvalues are determined by evaluating the Jacobian matrix partial derivatives at the E^0 coordinates.

$$E^0 = \left(\frac{f\Lambda_h}{(\psi + \mu_h)}, \frac{\Lambda_h(\psi + \mu_h - f\mu_h)}{\mu_h(\psi + \mu_h)}, 0,0,0,0, \frac{\Lambda_v}{\mu_v}, 0\right)$$

The Jacobian matrix obtained from equation (1)-(8) is as follows:

$$J(E^0) = \begin{bmatrix} -\psi - \mu_h & 0 & 0 & 0 & 0 & 0 & 0 & 0 \\ \psi & -\mu_h & 0 & 0 & 0 & \chi & 0 & -\frac{(1-\theta)\beta_h S_h^0}{N_v^0} \\ 0 & 0 & -\mu_h - \alpha & 0 & 0 & 0 & 0 & \frac{(1-\theta)\beta_h S_h^0}{N_v^0} \\ 0 & 0 & \alpha & -\mu_h - \delta_1 - \tau_1 - \sigma & 0 & 0 & 0 & 0 \\ 0 & 0 & 0 & \sigma & -\mu_h - \delta_2 - \tau_2 & 0 & 0 & 0 \\ 0 & 0 & 0 & \tau & 0 & -\chi - \mu_h & 0 & 0 \\ 0 & 0 & 0 & -\frac{\beta_v S_v^0}{N_h^0} & 0 & 0 & -\mu_v & 0 \\ 0 & 0 & 0 & \frac{\beta_v S_v^0}{N_h^0} & 0 & 0 & 0 & -\mu_v - \delta_v \end{bmatrix}$$

From this Jacobian matrix can be directly obtained five eigenvalues, which are explicitly written as:

$$\lambda_1 = -\psi - \mu_h, \lambda_2 = -\mu_h, \lambda_3 = -\mu_h - \delta_2 - \tau_2, \lambda_4 = -\chi - \mu_h, \lambda_5 = -\mu_v.$$

Since all biological parameters are strictly positive, the eigenvalues $\lambda_1, \lambda_2, \lambda_3, \lambda_4$, and λ_5 clearly have negative real parts. The remaining three eigenvalues λ_6, λ_7, and λ_8, which govern the primary host-vector disease transmission, are determined from a smaller sub-matrix block, yielding the following third-degree characteristic polynomial:

$$\lambda^3 + a_2\,\lambda^2 + a_1\,\lambda + a_0 = 0.$$

Where the polynomial coefficients a_2, a_1, and a_0 are derived from the trace and determinant properties of the remaining subsystem matrix:

$$a_2 = \mu_v + \delta_v + 2\mu_h + \delta_1 + \tau_1 + \sigma + \alpha, \quad (9)$$

$$a_1 = \alpha\delta_v + \alpha\delta_1 + \alpha\mu_v + \mu_h\,\alpha + \alpha\sigma + \alpha\tau_1 + \delta_v\delta_1 + 2\mu_h\,\delta_v + \delta_v\,\sigma + \delta_v\,\tau_1 + \delta_1\,\mu_v + \mu_h\,\delta_1 + 2\mu_h\,\mu_v + \mu_v\,\sigma + \mu_h^2 + \mu_h\,\sigma + \tau_1\alpha, \quad (10)$$

$$a_0 = \frac{1}{\psi + \mu_h}\,(-\alpha\beta_v\,\beta_h f\mu_h\theta + \alpha\beta_v f\mu_h + \alpha\beta_v\beta_h\,\mu_h\theta + \alpha\beta_v\beta_h\,\psi\theta - \alpha\beta_v\,\beta_h\,\mu_h - \alpha\beta_v\beta_h\,\psi + \alpha\delta_v\,\delta_1\,\mu_h + \alpha\delta_v\,\delta_1\psi + \alpha\delta_v\mu_h^2 + \alpha\delta_v\mu_h\psi + \alpha\delta_v\mu_h\sigma + \alpha\delta_v\mu_h\tau_1 + \alpha\delta_v\psi\sigma + \alpha\delta_v\psi\tau_1 + \alpha\delta_1\,\mu_v\mu_h + \alpha\delta_1 1\,\mu_v\,\psi +$$

$$\alpha\mu_v\mu_h^2 + \alpha\mu_v\mu_h\psi + \alpha\mu_v\mu_h\sigma + \alpha\mu_v\mu_h\tau_1 + \alpha\mu_v\psi\sigma + \alpha\mu_v\psi\tau_1 + \delta_v\delta_1\mu_h^2 + \delta_v\,\delta_1\,\psi + \mu_h^3 + \delta_v\,\mu_h^2\,\psi + \delta_v\,\mu_h^2\,\sigma + \delta_v\mu_h^2\tau_1 + \delta_v\mu_h\psi\sigma + \delta_v\mu_h\psi\tau_1 + \delta_1\mu_v\mu_h^2 + \delta_1\,\mu_v\,\mu_h\,\psi + \mu_v\mu_h^3 + \mu_v\mu_h^2\psi - \mu_v\,\mu_h^2\,\sigma + \mu_v\mu_h^2\,\tau_1 + \mu_v\,\mu_h\,\psi\sigma + \mu_v\,\mu_h\,\psi\tau_1), \quad (11)$$

Based on the Routh-Hurwitz criterion, the remaining eigenvalues λ_6, λ_7, and λ_8 possess negative real parts because the derived polynomial coefficients satisfy $a_2 > 0,\ a_0 > 0$ and $a_2a_1 - a_0 > 0$. Algebraically, $a_2 > 0$ is automatically satisfied since all biological parameters are positive, while a_0 remains strictly positive if and only if $R_0 < 1$, which concurrently guarantees the requirement $a_2\,a_1 - a_0 > 0$. This confirms that the disease-free equilibrium (E^0) is locally asymptotically stable when $R_0 < 1$. Conversely, if $R_0 > 1, E^0$ becomes unstable, and the system transitions to the endemic equilibrium (E^*).

An analytical Routh-Hurwitz proof for the endemic equilibrium is mathematically intractable due to the highly complex system of eight coupled nonlinear state variables. Instead, local stability was assessed numerically using Table 2 parameters; the resulting eigenvalues all possess strictly negative real parts, confirming local asymptotic stability. Consequently, this stability conclusion remains parameter-dependent rather than a general analytical proof for all biologically feasible values.

3.3 Basic Reproduction Number (R_0)

The basic reproduction number (R_0) is determined using the Next Generation Matrix (NGM) method. Focusing on the infected compartments: E_h, I_1, I_2 and I_v. Linearizing the system at the Disease-Free Equilibrium (DFE) yields the new infections (Matrix F) and the transition (Matrix V) are constructed as follows:

$$F = \begin{bmatrix} 0 & 0 & 0 & \frac{(1-\theta)\beta_h S_h}{N_v} \\ 0 & 0 & 0 & 0 \\ 0 & 0 & 0 & 0 \\ 0 & \frac{\beta_v S_v}{N_h} & 0 & 0 \end{bmatrix}, \text{ and } V = \begin{bmatrix} (\mu_h + \alpha) & 0 & 0 & 0 \\ -\alpha & (\mu_h + \delta_1 + \tau_1 + \sigma) & 0 & 0 \\ 0 & -\sigma & (\mu_h + \delta_2 + \tau_2) & 0 \\ 0 & 0 & 0 & (\mu_v + \delta_v) \end{bmatrix}.$$

The inverse of matrix V is constructed as follows:

$$V^{-1} = \begin{bmatrix} \frac{1}{\mu_h + \alpha} & 0 & 0 & 0 \\ \frac{\alpha}{(\mu_h + \alpha)(\mu_h + \delta_1 + \tau_1 + \sigma)} & \frac{1}{\mu_h + \delta_1 + \tau_1 + \sigma} & 0 & 0 \\ \frac{\alpha\sigma}{(\mu_h + \alpha)(\mu_h + \delta_1 + \tau_1 + \sigma)(\mu_h + \delta_2 + \tau_2)} & \frac{\sigma}{(\mu_h + \delta_1 + \tau_1 + \sigma)(\mu_h + \delta_2 + \tau_2)} & \frac{1}{\mu_h + \delta_2 + \tau_2} & 0 \\ 0 & 0 & 0 & \frac{1}{\mu_v + \delta_v} \end{bmatrix}$$

The R_0 is defined as the spectral radius of the next generation operator, $K = FV^{-1}$. By evaluating $\rho\,(FV^{-1})$, the basic reproduction number is explicitly given by:

$$R_0 = \rho\,(FV^{-1}) = \sqrt{\frac{\alpha(1-\theta)\beta_h\beta_v(\mu_h + \psi - f\mu_h)}{(\mu_h + \alpha)(\mu_v + \delta_v)(\mu_h + \delta_1 + \tau_1 + \sigma)(\psi + \mu_h)}}$$

As a threshold parameter, the basic reproduction number (R_0) determines the transmission potential of leptospirosis: if R_0<1, the disease-free equilibrium is stable and the infection gradually disappears, whereas if R_0>1, the disease persists. The obtained expression indicates that increasing the transmission rates β_h and β_v leads to a higher value of R_0, thereby enhancing disease spread. In contrast, increasing vaccination coverage (f), public awareness compliance (θ), and the recovery rate reduces the value of R_0, suggesting that these interventions play an important role in controlling leptospirosis transmission.

3.4 Numerical Simulation

Numerical simulations in MATLAB R2024a investigate leptospirosis transmission dynamics under vaccination and preventive behavioral interventions. Parameters are sourced from literature and official demographic reports, with remaining values estimated within biologically plausible ranges to initially simulate the Disease-Free Equilibrium (DFE) scenario.

Table 2. Parameter Values Used in Simulation

Parameter	Mark	Dimensions	Reference
Λ_h	20	/day	[6]
μ_h	0.02	/day	[6]
ψ	0.10	/day	[1]
f	0.80	dimensionless	[1]
β_h	0.10	/day	[30]
β_v	0.10	/day	[22]
α	0.25	/day	[4]
σ	0.15	/day	[1]
τ_1	0.10	/day	[31]
τ_2	0.047	/day	Assumed
δ_1	0.001	/day	[4]
δ_2	0.015	/day	[31]
δ_v	0.010	/day	[31]
χ	0.05	/day	[5]
θ	0.40	dimensionless	[1]
μ_v	0.02	/day	[12]
Λ_v	20	/day	calculated

Using MATLAB R2024a and the parameter values from Table 2, numerical simulations were conducted with initial condition $V(0) = 50,\ S_h(0) = 600,\ E_h(0) = 30, I_1(0) = 30, I_2(0) = 20,\ R_h(0) = 15,\ S_v = 800.\ I_v = 100.$ Evaluating the Jacobian matrix at the disease-free equilibrium (DFE) yields five negative eigenvalues: $\lambda_1 = -0.12, \lambda_2 = -0.02, \lambda_3 = -0.082,\ \lambda_4 = -0.07, \lambda_5 = -0.02,$ with the remaining stability governed by a third-order characteristic polynomial (9)-(11). The polynomial coefficients are calculated as $a_2 = 0.67, a_1 = 0.1416,$ and $a_0 = 0.0077.$ According to the Routh-Hurwitz criterion, since $a_2 > 0, a_0 > 0,$ and $a_2 a_1 - a_0 = 0.0871 > 0,$ it is guaranteed that the remaining three eigenvalues also have negative real parts. Consequently, with $R_0 = 0.7696 < 1,$ the DFE is proven to be locally asymptotically stable. Conversely, the parameter values in Table 2 were used with modification were made to $f = 0.15, \beta_h = 0.66, \theta = 0.10$ and based on calculation result using Routh-Hurwitz criteria, the basic reproduction number is $R_0 = 6.009.$ Evaluating the Jacobian matrix at the endemic equilibrium using the parameters in Table 2 yields eigenvalues with strictly negative real parts, numerically confirming its local asymptotic stability.

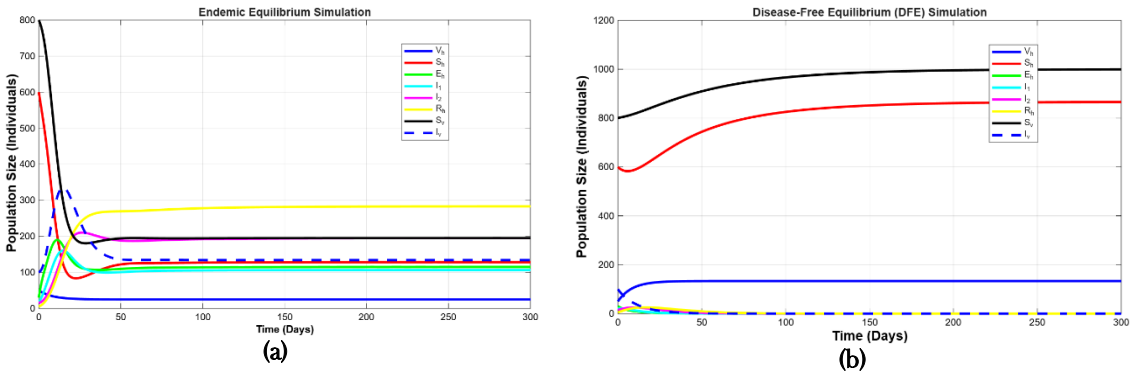

Figure 2. Numerical simulation of the leptospirosis model over time showing.
Panel (a) shows trajectories approaching the endemic equilibrium (EE).
Panel (b) shows trajectories approaching the disease-free equilibrium (DFE).

Numerical simulations were conducted over a 300-day period using the parameters listed in Table 2 to validate the analytical results (Figure 2). In figure 2(a), demonstrates the model trajectories approaching the endemic equilibrium (EE). Following a brief transient period, all state variables specifically the infected and exposed compartments $(E_h, I_1, I_2, and\ I_v)$ stabilize at constant positive values, confirming permanent disease

persistence in both human and vector populations. Meanwhile, figure 2(b) illustrates the trajectories approaching the disease-free equilibrium (DFE). In this scenario, the exposed, early-stage infected, severe-stage infected, and infected vector populations gradually decay to zero, while the vaccinated and susceptible populations stabilize at their non-zero steady-state levels. These numerical outcomes are fully consistent with the analytical stability properties established for both equilibria.

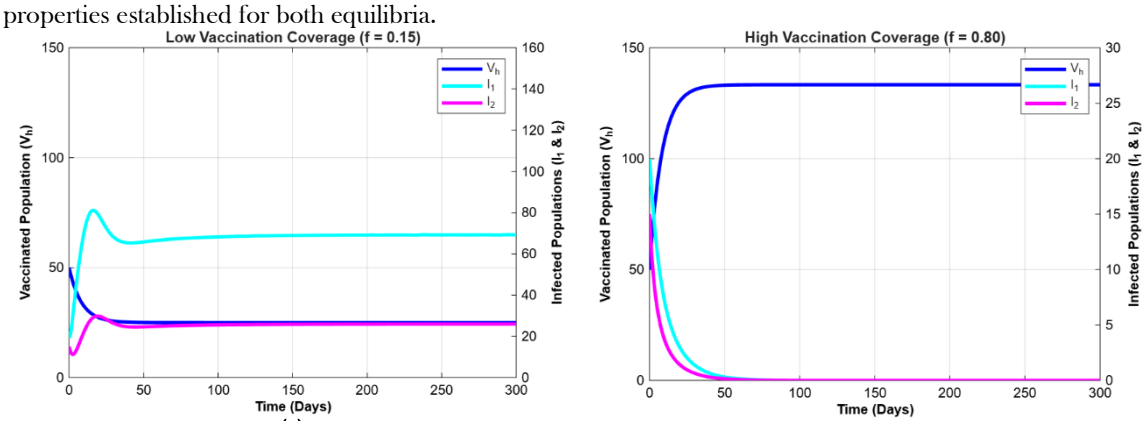

Figure 3. Impact of vaccination coverage on leptospirosis dynamics.
Panel (a) shows low vaccination rate $(f = 0.15)$.
Panel (b) shows high vaccination rate $(f = 0.80)$.

Figure 3 illustrates the impact of vaccination coverage (f) on leptospirosis dynamics. In Figure 3(a), low coverage $(f = 0.15)$ fails to suppress transmission, allowing both infected classes (I_1 and I_2) to persist. Conversely, increasing coverage to to $f = 0.80$ in Figure 3(b) rapidly elevates the vaccinated population and drives both infected classes toward zero, demonstrating that vaccination effectively prevents new infections and limits clinical progression to severe stages. Rather than conducting an exhaustive sweep, these two representative scenarios illustrate the qualitative transition between disease persistence and elimination, leaving a broader exploration of vaccination (f) and public awareness (θ) for future work. Ultimately, higher vaccination coverage is shown to be highly effective in driving the system toward a disease-free state.

3.5 Sensitivity Analysis of R_0

By substituting the parameter values from Table 2 into the analytical derivative formulas, the numerical sensitivity indices for R_0 are obtained. The calculation results and their corresponding magnitude rankings are summarized in Table 3.

Table 3. Sensitivity indices of model parameters relative to R_0

Parameter	Mark	Sensitivity Index
μ_h	0.02	-0.1380
ψ	0.10	+0.0370
f	0.80	-0.0769
β_h	0.10	+0.50000
β_v	0.10	+0.50000
α	0.25	+0.0370
σ	0.15	-0.2768
τ_1	0.10	-0.1845
δ_1	0.001	-0.0018
δ_v	0.010	-0.1667
θ	0.40	-0.3333
μ_v	0.02	-0.3333

The sign of the sensitivity index determines the proportional relationship between the model parameters and the basic reproduction number (R_0). where positive and negative signs indicate direct and inverse proportions, respectively. Host-vector transmission rates (β_h and β_v) exert the strongest positive impact of $(+0.5000)$, where a 10% increase raises R_0 by 5%, thereby amplifying the transmission potential of leptospirosis. Other parameters showing positive correlations include the environmental carrier rate $(\psi = +0.0641)$ and the transition rate to the infectious class $(\alpha = +0.0370)$. Conversely, parameters with negative indices share an inverse relationship with R_0 and serve as inhibitors of the epidemic. The public awareness compliance rate (θ) and the natural vector mortality rate (μ_v) yield the highest negative sensitivity index of -0.3333.

Epidemiologically, a 10% improvement in public behavioral adherence or vector control interventions will reduce R_0 by 3.33%. Additionally, the clinical isolation rate of the severe stage ($\sigma = -0.2768$) and the recovery rate of the first infectious stage ($\tau_1 = -0.1845$) also demonstrate substantial mitigation capabilities. Under the current baseline scenario, the vaccination coverage ($f = -0.0769$) and the natural human mortality rate ($\mu_h = -0.1380$) show minor relative mitigation effects on the threshold parameter.

3.6 Discussion

The proposed stage-structured model confirms that the basic reproduction number R_0 governs the local stability of the disease-free (E^0) and endemic (E^*) equilibria. While previous leptospirosis models proposed by Eguda et al. [1] and Engida et al. [4] primarily represented human infection using a single infectious compartment, the present study integrates temporary vaccination with waning immunity and a two-stage clinical progression into a unified analytical framework.

Although contact rates (β_h, β_v) primary drives of R_0, numerical results demonstrate that combining vaccination (f) and public awareness compliance (θ) effectively suppresses infection levels. Specifically, weakening these interventions (reducing f to 0.15, increasing β_h to 0.66, and lowering θ to 0.10) causes R_0 to rise 6.009, severely worsening endemic conditions. From a public health perspective, these findings highlight the necessity of integrated mitigation measures: sustained high vaccination coverage ($f \geq 0.80$) must be paired with strong community adherence to preventive practices, timely medical treatment, environmental sanitation, and active rodent control programs to disrupt transmission pathways in endemic areas.

This study provides qualitative theoretical insights under constant transmission rates rather than exact empirical predictions. Due to the high dimensionality of the eight-dimensional nonlinear system, analytical proofs for the local stability of the endemic equilibrium and global asymptotic stability (GAS) are mathematically intractable. The complex host-vector cross-transmission feedback loops prevent standard linear or Volterra-type Lyapunov functions from achieving definitive negative semi-definiteness, requiring local stability to be verified numerically. Future research will focus on calibrating the model against empirical epidemiological data and incorporating seasonal hydroclimatic variables, such as rainfall and flooding frequencies, to better evaluate long-term leptospirosis dynamics.

4. CONCLUSION

This study developed a stage-structured compartmental model integrating temporary vaccine-induced immunity and two-stage clinical treatments for leptospirosis. The analytical framework confirms that long-term transmission dynamics are governed by the basic reproduction number R_0, where reducing $R_0 < 1$ ensures the local stability of the disease-free equilibrium and pathogen eradication. Numerical simulations executed in MATLAB using baseline parameters yielded $R_0 = 0.7696$, demonstrating that high vaccination coverage and strong public awareness compliance can successfully eliminate the infection. Conversely, weakening these interventions ($f = 0.15, \beta_h = 0.66, and\ \theta = 0.10$) drives R_0 up to 6.009, causing the disease to persist endemically.

Because human leptospirosis vaccines are not currently deployed at scale, the high-coverage simulation serves as a theoretical counterfactual to establish the mathematical bounds of potential immunization. Since the vaccine is not an active policy option, practical public health strategies must prioritize immediate environmental sanitation and rodent control to suppress the dominant transmission rate β_h. Crucially, because this framework utilizes literature-based parameters, these mathematical findings offer qualitative theoretical insights into transmission dynamics rather than exact epidemiological predictions. Consequently, these results should be interpreted by policy-makers as strategic guidelines for designing integrated interventions rather than precise quantitative forecasts.

While this study provides essential baseline dynamics, it is restricted to local stability analysis under constant transmission rates without empirical calibration. Future research will address these limitations by developing global asymptotic stability proofs, executing parameter estimation using real-world surveillance data, and incorporating seasonal hydroclimatic factors such as rainfall and flooding frequencies to enhance the predictive capability and practical applicability of the model.

5. REFERENCES

[1] F. Y. Eguda, A. M. Shuaiba, O. C. Ameh, S. E. Abah, S. M. Mohammed, and I. S. Mohammed, "Mathematical model for the transmission dynamics of Leptospirosis in human population," *Gadau J. Pure Allied Sci.*, vol. 2, no. 1, pp. 58–75, Apr. 2023, doi: 10.54117/gjpas.v2i1.66.

[2] A. Khan, G. Hussain, and G. Zaman, "Global dynamics and sensitivity analysis of a zoonotic leptospirosis model with environmental influence," *J. Appl. Math. Comput.*, vol. 70, no. 1, pp. 123–145, 2024, doi: 10.1007/s12190-023-01912-1.

[3] E. A. Bradley and G. Lockaby, "Leptospirosis and the Environment: A Review and Future Directions," *Pathogens*, vol. 12, no. 9, p. 1167, Sep. 2023, doi: 10.3390/pathogens12091167.

[4] H. A. Engida, D. M. Theuri, D. Gathungu, J. Gachohi, and H. T. Alemneh, "A Mathematical Model Analysis for the Transmission Dynamics of Leptospirosis Disease in Human and Rodent Populations," *Comput. Math. Methods Med.*, vol. 2022, pp. 1–23, Sep. 2022, doi: 10.1155/2022/1806585.

[5] R. Artiono *et al.*, "Mathematical Analysis and Numerical Simulation on Free-Living Leptospira: A Mathematical Modeling Perspective," *Eur. J. Pure Appl. Math.*, vol. 17, no. 3, pp. 1637–1658, Jul. 2024, doi: 10.29020/nybg.ejpam.v17i3.5178.

[6] Ministry of Health of the Republic of Indonesia, "Indonesia Health Profile 2023," Jakarta: Ministry of Health of the Republic of Indonesia, 2024.

[7] Ministry of Health of the Republic of Indonesia, "Leptospirosis Situation in Indonesia 2024," Jakarta: Ministry of Health, 2024.

[8] World Health Organization Indonesia, "Integrated Leptospirosis Surveillance Through a One Health Approach," Jakarta: WHO Indonesia, 2022.

[9] BPS-Statistics Indonesia, "Statistical Yearbook of Indonesia 2023," Jakarta: BPS-Statistics Indonesia, 2023.

[10] M. A. Gallego and M. V. Simoy, "Mathematical modeling of leptospirosis: A dynamic regulated by environmental carrying capacity," *Chaos, Solitons & Fractals*, vol. 152, p. 111425, Nov. 2021, doi: 10.1016/j.chaos.2021.111425.

[11] M. Sooryadas, A. L. Haseena, S. Selsha, and K. Balachandran, "Stability analysis of leptospirosis compartmental model with impact of contaminated environment," *Nonlinear Anal. Model. Control*, vol. 30, no. 5, pp. 957–981, Aug. 2025, doi: 10.15388/namc.2025.30.42973.

[12] S. Olaniyi, O. S. Oladipo, and K. O. Okosun, "Mathematical modeling of leptospirosis transmission dynamics with environmental reservoir and vector control," *Theor. Biol. Med. Model.*, vol. 19, no. 1, p. 14, 2022, doi: 10.1186/s12976-022-00168-w.

[13] S. Møgelmose, K. Neels, and N. Hens, "Incorporating human dynamic populations in models of infectious disease transmission: a systematic review," *BMC Infect. Dis.*, vol. 22, no. 1, p. 862, Nov. 2022, doi: 10.1186/s12879-022-07842-0.

[14] S. Chadsuthi and C. Modchang, "Mathematical modeling of leptospirosis transmission with hydroclimatic factors and assessing the control strategies," *Sci. Rep.*, vol. 11, no. 1, p. 15303, 2021, doi: 10.1038/s41598-021-94646-x.

[15] A. G. Regassa and L. L. Obsu, "The role of asymptomatic cattle for leptospirosis dynamics in a herd with imperfect vaccination," *Sci. Rep.*, vol. 14, no. 1, p. 23775, Oct. 2024, doi: 10.1038/s41598-024-72613-7.

[16] D. A. Haake and P. N. Levett, "Leptospirosis in Humans," in *Current Topics in Microbiology and Immunology*, 2015, pp. 65–97. doi: 10.1007/978-3-662-45059-8_5.

[17] Antima and S. Banerjee, "Modeling the dynamics of leptospirosis in India," *Sci. Rep.*, vol. 13, no. 1, p. 19791, Nov. 2023, doi: 10.1038/s41598-023-46326-2.

[18] M. Roccetti, "Predictive health intelligence: Potential, limitations and sense making," *Math. Biosci. Eng.*, vol. 20, no. 6, pp. 10459–10463, 2023, doi: 10.3934/mbe.2023460.

[19] L. M. Bilung *et al.*, "Leptospira and Leptospirosis: A Review of Species Classifications, Genomes, Morphological Structures, Antimicrobial Resistances, Transmissions, and Clinical Manifestations," *Curr. Microbiol.*, vol. 83, no. 2, p. 122, Feb. 2026, doi: 10.1007/s00284-026-04722-7.

[20] World Health Organization, "Human Leptospirosis: Guidance for Diagnosis, Surveillance and Control," World Health Organization, Geneva, Switzerland, 2021.

[21] A. Ayalew, Y. Molla, T. Tilahun, and T. Tesfa, "Mathematical Model and Analysis on the Impacts of Vaccination and Treatment in the Control of the COVID-19 Pandemic with Optimal Control," *J. Appl. Math.*, vol. 2023, pp. 1–15, Mar. 2023, doi: 10.1155/2023/8570311.

[22] V. Saravanan, R. Chinnathambi, and F. A. Rihan, "Modeling and controlling Leptospirosis transmission in humans and rodents," *J. Math. Comput. Sci.*, vol. 39, no. 01, pp. 30–49, Mar. 2025, doi: 10.22436/jmcs.039.01.03.

[23] X. Guo *et al.*, "Computing R0 of dynamic models by a definition-based method," *Infect. Dis. Model.*, vol. 7, no. 2, pp. 196–210, Jun. 2022, doi: 10.1016/j.idm.2022.05.004.

[24] A. F. Brouwer, "Why the Spectral Radius? An intuition-building introduction to the basic reproduction number," *Bull. Math. Biol.*, vol. 84, no. 9, p. 96, Sep. 2022, doi: 10.1007/s11538-022-01057-9.

25] J. H. Choi, H. M. Lee, and S. Y. Kim, "Treatment failure and the threshold of disease extinction," *Math. Biosci.*, vol. 377, p. 109302, Nov. 2025, doi: 10.1016/j.mbs.2024.109302.
[26] Antima and S. Banerjee, "Understanding the dynamics and drivers of leptospirosis in tropical and subtropical regions: a mathematical and epidemiological approach," *Nonlinear Dyn.*, vol. 113, no. 9, pp. 10705–10727, May 2025, doi: 10.1007/s11071-024-10767-9.
[27] S. Bilal, M. I. Khan, and A. Riaz, "Mathematical study of infectious disease dynamics with multi-compartment structure and stability criteria," *Rend. del Circ. Mat. di Palermo Ser. 2*, vol. 72, no. 4, pp. 2345–2362, 2023, doi: 10.1007/s12215-022-00812-4.
[28] H. A. Engida, "Analysis of a Comprehensive Mathematical Model for Leptospirosis Dynamics: An Optimal Control Application," *J. Math.*, vol. 2025, no. 1, p. 7338974, Jan. 2025, doi: 10.1155/jom/7338974.
[29] O. J. Peter, K. O. Adebayo, and F. A. Oguntolu, "On the endemic persistence of vector–host infectious diseases under control interventions," *Int. J. Biomath.*, vol. 17, no. 3, p. 2350041, 2024, doi: 10.1142/S179352452350041X.
[30] X. Shi, D. Zhou, X. Zhou, and F. Yu, "Predicting the trend of leptospirosis in China via a stochastic model with vector and environmental transmission," *Electron. Res. Arch.*, vol. 32, no. 6, pp. 3937–3951, 2024, doi: 10.3934/era.2024176.
[31] D. Savitri, M. Jakfar, and A. Suryanto, "Dynamical analysis of a leptospirosis model considering host vaccination and vector population dynamics," *Chaos, Solitons & Fractals*, vol. 158, p. 112045, 2022, doi: 10.1016/j.chaos.2022.112045.